American Mineralogist, Volume 82, pages 1007–1013, 1997

Refinement of the cookeite "*r*" structure

Hong Zheng* and Sturges W. Bailey†

Department of Geology and Geophysics, 1215 West Dayton Street, University of Wisconsin, Madison, Wisconsin 53706, U.S.A.

Abstract

The rare two-layer "*r*" structure of I*aa* cookeite from Little Rock, Arkansas, was refined in space group *Cc* to $R = 7.1\%$. Mean T-O bond lengths of 1.654(1) Å and 1.657(1) Å in one tetrahedral sheet vs. 1.659(1) Å and 1.685(1) Å in the other sheet indicate a partly ordered but asymmetric distribution of tetrahedral Si and Al. The two tetrahedral sheets within the 2:1 layer have different compositions and charges. The Al-rich, higher-charge tetrahedral sheet is thicker and has a closer approach to the interlayer sheet than does the Si-rich, lower-charge sheet. Two Al cations occupy the cis octahedra in the dioctahedral 2:1 layer. Mean M-O,OH bond lengths of 1.946(1), 1.946(1), and 2.110(1) Å in the trioctahedral interlayer sheet indicate a partly ordered distribution of octahedral Al and Li. The Li-rich, lower-charge octahedron in the interlayer is located on a vertical straight line between an Al-rich tetrahedron and a Si-rich tetrahedron. The two higher-charge interlayer Al are located vertically between a Si-rich tetrahedron and the center of a six-membered ring. This pattern of ordering minimizes the cation-cation repulsion inherent in a I*aa* structure and gives the best local charge balance. The protons of the six surface OH groups tilt away from the two Al-rich interlayer sites toward the lower-charge Li site. The details of the interlayer hydrogen bond contacts are influenced by the ordering patterns and the structural distortions present.

Introduction

Cookeite is a di,trioctahedral chlorite in which the 2:1 layer is dioctahedral and the hydroxide interlayer is trioctahedral. It is a common alteration product of Li-bearing minerals in pegmatites and hydrothermal veins and may precipitate directly from hydrothermal solutions as well. Černý (1970), in a study of the most reliable chemical analyses of cookeite, found that tetrahedral Al was nearly constant at 3.0 Si per 4.0 positions, but with tetrahedral Al of some specimens substituted by small amounts of B or Be. Li ranges between 0.8 and 1.4 atoms per formula unit and is concentrated mainly in the interlayer sheet. Small amounts of Ca, Na, and K are often reported in chemical analyses of dioctahedral chlorites as cations residing between the 2:1 layers and the interlayer sheet. However, they are more likely to be impurities according to Peacor et al. (1988). The total octahedral occupancy ranges between 4.8 and 5.3 atoms per 6.0 sites in the formulae of Černý (1970), but if the Ca, Na, and K are excluded as impurities, both the total occupancy and individual atom values require small revisions. An ideal composition is $Al_2(Si_3Al)O_{10}(OH)_2 \cdot (Al_2Li)(OH)_6$.

From surveys of many cookeite specimens, Bailey and Brown (1962) and Bailey and Lister (1989) reported that by far the great majority of specimens are based on I*a* units. The two known exceptions are II*b* specimens from pegmatites at Dobrá Voda, Macedonia, and Norway, Maine. Bailey and Lister (1989) found that most of the cookeite rosettes in Li-bearing pegmatites appear to be imperfect two-layer structures similar to the monoclinic "*s*" structure derived by Mathieson and Walker (1954) in a study of vermiculite. A better crystallized two-layer cookeite was reported by Bailey and Lister (1989) from Wait-a-bit Creek, British Columbia, and at several localities in and around Little Rock, Arkansas. The latter include cookeite from the Jeffrey quarry, which is part of the Source Clays Repository of The Clay Minerals Society. The structure can be correlated with the monoclinic "*r*" and "*q*" structures of Mathieson and Walker (1954). These two structures are enantiomorphic in space group *Cc*. Bailey (1975) summarized results of an incomplete structural refinement of one of the Little Rock crystals. In that structure, Li was found to be ordered in one interlayer site where it achieves the best local charge balance. Interlayer Li^{1+} lies on a vertical line directly between a tetrahedral cation in the 2:1 layer below and a tetrahedral cation in the 2:1 layer above. The more highly charged interlayer Al^{3+} cations, however, only have a tetrahedral cation on one side and the center of a six-membered ring on the other side. Although different T-O bond lengths were determined during the structural refinement, the poor quality of the film data did not permit a firm conclusion as to ordering of tetrahedral Si and Al. The refinement implies, however, that the two sides of the 2:1 layer may have different tetrahedral compositions and charges.

* Present address: 8109 West 96th Street, Bloomington, MN 55438, U.S.A.

† Deceased November 30, 1994.

0003–004X/97/0910–1007$05.00

Table 1. Electron microprobe analysis

Oxide	wt%	Atoms	
SiO_2	34.31	Si	3.042
Al_2O_3	47.62	Al	4.975
FeO	0.13	Fe	0.009
Cr_2O_3	0.07	Cr	0.005
MgO	0.05	Mg	0.007
K_2O	0.01	K	0.001
CaO	nil	Ca	0
NaO	nil	Na	0
Li_2O*	2.39	Li	0.850
H_2O	15.42		
Σ	100.00		

Notes: Analyst: J. Fournelle. Cameca SX50 no. 485 operated at 15 kV and 20 nA; fixed beam. Standards = forsterite, anorthite, fayalite, nickel. Absorption corrections by PAP ($\phi\rho Z$) method. Atoms based on assumption of 28 positive charges.

* Li_2O by neutron activation.

The present paper reports a further study of the Arkansas cookeite. Stone and Milton (1976) identified cookeite in small hydrothermal quartz veins in the Jackfork Sandstone of Mississippian and Pennsylvanian ages. The cookeite occurrences cover an E-W distance of nearly 50 miles near the intersection of the Frontal Ouachitas with the Gulf Coastal Plain at Little Rock, Arkansas, approximately 70 miles NE of Magnet Cove. Charles G. Stone of the Arkansas Geological Commission kindly supplied samples of 11 quartz-cookeite veins in and around Little Rock and North Little Rock. All of these cookeite samples were I*a* "*r*" or "*q*" polytypes. Thus, there appears to be a regional geochemical significance to this otherwise rare structure. The largest crystals, up to 1.0 cm in diameter, were from a quartz vein in a railroad cut near the intersection with 13th Street in Little Rock. A crystal from this locality was selected for structural refinement (U.W. Geological Museum No. 6003/5).

The purpose of this study was to obtain a better refinement than that in the earlier film study and thereby to focus on (1) the pattern and extent of cation ordering, (2) the validity of an asymmetric charge distribution on the two sides of the 2:1 layer, and (3) the positions of the protons associated with the OH groups.

Experimental methods

Cookeite crystals free of impurities were hand-picked under a binocular microscope for chemical analysis. Major elements were determined by electron microprobe and Li by nuclear activation (Table 1). The resulting structural formula based on 28 cationic charges is $Al_{2.0}(Si_{3.042}Al_{0.958})O_{10}(OH)_2(Al_{2.017}Li_{0.852}Cr_{0.005}Mg_{0.007}Fe_{0.009}\square_{0.110})(OH)_6$, neglecting a small amount of K. The H_2O, by difference, is equivalent to $(OH)_{7.98}$.

Although the crystals are macroscopically planar, the (001) surfaces tend to be slightly corrugated, and all crystals examined exhibited some mosaic spread in the individual X-ray reflections. There was no streaking between $k \neq 3n$ reflections, however, and a crystal with the smallest mosaic spread was selected for further study. This crystal measured 0.35 × 0.31 × 0.05 mm. Unit cell dimensions of a = 5.158(1), b = 8.940(2), c = 28.498(6) Å, β = 96.60(3)°, and V = 1305(1) Å^3 were obtained by least-squares refinement of 30 centered reflections on a single-crystal diffractometer. The 2θ values of these reflections were in the range from 41.0° to 62.4° with monochromatic Mo$K\alpha$ X-radiation. No violations of the systematic absences for space group *Cc* were detected. Initially, intensity data sets were collected with monochromatic Mo$K\alpha$ X-radiation using both θ-2θ and ω scans, each corrected for absorption by both semi-empirical ψ scans and analytical shape-correction techniques. Because of the large c repeat and the mosaic spread, reflection overlap occurred in all four data sets. A fifth data set, collected with monochromatic Cu$K\alpha$ X-radiation, avoided overlap but registered only one-half the total number of diffractions that had been collected with Mo X-radiation. Partial refinement of all five data sets showed that the smallest errors and best displacement factors were from the data set taken with Mo$K\alpha$ X-radiation, θ-2θ scans, and corrected for absorption by the analytical shape-correction technique. Only the results from refinement of this data set are reported here.

The intensities of 5828 reflections were measured using θ-2θ scans with a Siemens P4 rotating-anode single-crystal diffractometer at a power setting of 15 kW (50 kV, 300 mA). The variable scan speeds were 2° to 20°/min in 2θ, varying as a function of intensity, with a scan width of 2° in 2θ. Intensity data for 2θ values between 3.5° and 60° were collected in all octants, then merged into 1899 independent reflections. The intensities of two standard reflections were measured every 98 reflections to monitor crystal and electronic stability. No instability was found. The raw data were corrected for absorption by the analytical shape-correction technique and for Lorentz and polarization factors.

Structure determination and refinements

Bailey (1975) determined the structure of this cookeite specimen as the two-layer enantiomorphic I*a* "*r*" or "*q*" structures described by Mathieson and Walker (1954) in their study of vermiculite. We verified this structure from precession photographs. We chose to use the "*r*" structure and positioned the cations according to the positions determined by Bailey (unpublished data). The positions of the anions were determined by the probability method for phase angles using program SHELXL-93 followed by E maps. Subsequent refinement by least-squares assumed complete disorder of Si and Al within the two tetrahedral sheets and of Al and Li within the octahedral interlayer sheets in space group *Cc*, with the cation occupancy values constrained to the composition given by the chemical analysis. Reflections were assigned unit weights and a single scale factor. The atomic displacement factors were initially limited to be isotropic. As the refinement progressed, scale factor, atomic positions, and cation occupancies were allowed to vary, and the atomic displacement factors were refined anisotropically. Refinements stopped at a residual R of 7.6%. The difference electron

TABLE 2. Atomic coordinates and anisotropic displacement factors

Atom	x/a	y/b	z/c	U_{equiv}	U_{11}	U_{22}	U_{33}	U_{23}	U_{13}	U_{12}
Al1	0.4916(6)	0.5004(7)	0.0001(2)	0.005(1)	0.0024(6)	0.0029(6)	0.0096(7)	0.0005(6)	0.0015(6)	−0.0003(7)
Al2	0.4896(6)	0.8368(6)	0.0000(3)	0.015(1)	0.0146(6)	0.0144(6)	0.0175(7)	−0.0002(7)	0.0022(7)	0.0002(7)
Al3	0.5017(5)	−0.0051(6)	0.2502(2)	0.017(2)	0.0165(7)	0.0165(7)	0.0186(6)	0.0000(7)	0.0022(7)	0.0000(6)
Al4	0.5023(5)	0.3243(6)	0.2502(3)	0.012(1)	0.0107(7)	0.0105(6)	0.0139(7)	0.0000(7)	0.0020(7)	0.0003(6)
Li	0.5005(6)	0.6681(6)	0.2509(2)	0.007(3)	0.0070(7)	0.0069(7)	0.0069(6)	0.0000(6)	0.0007(7)	−0.0001(6)
T1	0.3885(6)	−0.0114(6)	0.0959(3)	0.015(1)	0.0139(6)	0.0142(6)	0.0184(7)	−0.0002(7)	0.0026(7)	−0.0002(7)
T2	0.4001(5)	0.6570(6)	0.0956(2)	0.012(1)	0.0102(7)	0.0100(6)	0.0152(6)	−0.0001(7)	0.0023(6)	−0.0009(7)
T3	0.5868(6)	0.3282(7)	0.4048(2)	0.030(2)	0.0293(6)	0.0293(7)	0.0311(7)	−0.0004(6)	0.0037(6)	0.0006(6)
T4	0.5954(5)	0.6580(7)	0.4041(2)	0.005(1)	0.0021(7)	0.0024(6)	0.0098(7)	0.0000(6)	0.0021(6)	0.0005(7)
O1	0.1127(6)	0.6158(7)	0.1130(3)	0.037(6)	0.0371(7)	0.0372(6)	0.0375(6)	−0.0001(7)	0.0045(7)	0.0001(7)
O2	0.4818(6)	0.8234(7)	0.1184(3)	0.022(4)	0.0220(7)	0.0221(7)	0.0226(7)	0.0007(7)	0.0026(7)	0.0000(7)
O3	0.6277(7)	0.5417(8)	0.1203(4)	0.023(5)	0.0232(7)	0.0233(6)	0.0238(7)	0.0001(7)	0.0029(7)	0.0000(7)
O4	0.3203(6)	−0.0261(8)	0.0381(4)	0.018(4)	0.0173(6)	0.0175(6)	0.0182(7)	0.0000(7)	0.0022(7)	−0.0001(7)
O5	0.4050(6)	0.6684(7)	0.0378(4)	0.022(5)	0.0220(6)	0.0222(6)	0.0227(7)	0.0000(7)	0.0027(7)	0.0000(7)
O6	0.3649(7)	0.2095(7)	0.3799(4)	0.023(4)	0.0227(6)	0.0230(6)	0.0234(7)	−0.0001(7)	0.0028(7)	0.0000(7)
O7	0.5112(6)	0.4910(7)	0.3791(3)	0.029(5)	0.0283(6)	0.0283(6)	0.0289(6)	0.0001(7)	0.0032(8)	0.0000(7)
O8	0.8632(6)	0.2822(7)	0.3839(3)	0.026(5)	0.0261(7)	0.0264(7)	0.0269(6)	0.0000(7)	0.0033(8)	0.0000(7)
O9	0.5840(6)	0.3319(7)	0.4631(3)	0.004(3)	0.0033(7)	0.0039(6)	0.0051(7)	0.0001(7)	0.0010(8)	0.0003(7)
O10	0.6555(7)	0.6424(8)	0.4631(3)	0.010(3)	0.0097(6)	0.0097(7)	0.0106(6)	0.0002(7)	0.0015(8)	−0.0001(7)
OH1	0.3243(7)	0.3586(8)	0.0373(4)	0.008(3)	0.0074(7)	0.0069(7)	0.0083(6)	−0.0001(7)	0.0010(8)	0.0002(7)
OH2	0.6567(6)	0.0197(7)	0.4628(3)	0.006(3)	0.0054(7)	0.0055(7)	0.0065(7)	0.0000(7)	0.0011(8)	−0.0003(7)
OH3	0.1528(6)	−0.0150(8)	0.2157(3)	0.020(4)	0.0204(6)	0.0204(7)	0.0206(6)	0.0000(7)	0.0022(7)	−0.0002(7)
OH4	0.1604(7)	0.3429(8)	0.2142(3)	0.009(3)	0.0082(6)	0.0084(6)	0.0090(7)	0.0000(7)	0.0009(8)	0.0001(7)
OH5	0.1230(6)	0.6595(7)	0.2138(4)	0.009(3)	0.0089(7)	0.0085(7)	0.0092(6)	−0.0001(6)	0.0013(8)	0.0001(7)
OH6	0.3820(7)	0.1594(7)	0.2868(4)	0.017(4)	0.0164(7)	0.0164(7)	0.0169(7)	−0.0001(7)	0.0021(7)	−0.0001(7)
OH7	0.3497(6)	0.4827(7)	0.2849(3)	0.035(6)	0.0345(6)	0.0346(7)	0.0347(7)	0.0000(7)	0.0041(8)	0.0001(7)
OH8	0.3409(7)	0.8452(7)	0.2872(3)	0.028(5)	0.0283(6)	0.0282(6)	0.0285(7)	0.0001(7)	0.0033(8)	0.0000(7)
H1	0.387	0.317	0.068							
H2	0.535	−0.002	0.436							
H3	0.131	−0.011	0.182							
H4	0.140	0.338	0.179							
H5	0.106	0.658	0.181							
H6	0.378	0.184	0.320							
H7	0.376	0.489	0.319							
H8	0.366	0.839	0.322							

Note: The positions of H1 through H8 obtained from difference electron density map and not refined.

density (DED) maps at this stage were flat at all atomic positions and did not reveal any obviously wrong atomic positions or extra maxima that might indicate twinning or an intergrowth of structures. The final cation occupancies are consistent with the ordering pattern found by Bailey (1975).

Comparison of F_o and F_c showed several rows of indices differing only in ℓ values in which the F_o values were consistently and significantly smaller or larger than the F_c values. We deleted about 200 reflections of this type, which were probably affected by overlap. Further refinement stopped at R = 7.1%, but we did not feel justified in deleting more data.

Bond lengths appear quite reasonable with small errors, and the anisotropic atomic displacement factors were small. A residual R of 7.1% may indicate a lower symmetry than *Cc* and resultant averaging of atomic sites. However, we could find no violations of the systemic absences required by *Cc* symmetry. Inspection of DED maps allowed identification of peak regions within which the protons associated with all eight OH groups are close to the predicted positions. Calculations produced local maxima of the interpolated peak DED surfaces. These maxima were taken as the proton positions and were not further refined. This is usually not possible with R = 7.1%. We conclude that the high R value is due to the overlap of reflections caused by the mosaic spread and large c repeat of 28.5 Å, and that the basic structure is reliable.

Table 2 lists the final atomic positions and anisotropic U values. Table 3 contains bond lengths and angles with errors as calculated by program ORFFE (Busing et al. 1964). Table 4 is a summary of some important structural features. Table 5 lists H distances and angles.

OCTAHEDRAL CATION ORDERING

The ordered distribution of interlayer Li^{1+} and Al^{3+} found in this study is similar to that reported by Bailey (1975) from an incomplete refinement (R = 10.3%) using film techniques. The lower-charge Li^{1+} is concentrated primarily in the only octahedral interlayer site that is located on a vertical straight line between tetrahedral cations directly below and above. The higher-charge Al^{3+} cations are located in the two interlayer sites where they lie vertically between a tetrahedral cation on only one side and the center of a six-membered ring on the other side. This distribution minimizes the cation-cation repulsion inherent in an I*a* structure and gives the best local charge balance. Refinement of the occupancies of the three interlayer octahedral sites gave $Li_{0.82}Al_{0.18}$, $Al_{0.91}Li_{0.09}$, and $Al_{0.91}Li_{0.09}$ (Table 4). The mean M-O,OH bond length of the Li-rich site is 2.110 Å compared with

TABLE 3. Bond lengths (Å) and angles (°)

T1-O1	1.655(1)	O4*-O1	2.776(2)	O4*-T1-O1	114.23(4)
T1-O2	1.659(1)	O4*-O2	2.704(2)	O4*-T1-O2	109.54(4)
T1-O3	1.652(1)	O4*-O3	2.718(2)	O4*-T1-O3	110.60(4)
T1-O4*	1.650(1)	O1-O2	2.708(1)	O1-T1-O2	109.60(4)
Mean	1.654(1)	O1-O3	2.619(1)	O1-T1-O3	104.70(4)
		O2-O3	2.678(1)	O2-T1-O3	107.90(4)
		Mean	2.701(1)	Mean	109.43(2)
T2-O1	1.659(1)	O5*-O1	2.800(2)	O5*-T2-O1	115.42(4)
T2-O2	1.659(1)	O5*-O2	2.674(2)	O5*-T2-O2	107.71(4)
T2-O3	1.657(1)	O5*-O3	2.740(2)	O5*-T2-O3	111.73(4)
T2-O5*	1.653(1)	O1-O2	2.651(2)	O1-T2-O2	106.07(4)
Mean	1.657(1)	O1-O3	2.722(2)	O1-T2-O3	110.36(4)
		O2-O3	2.627(1)	O2-T2-O3	104.79(4)
		Mean	2.702(1)	Mean	109.35(2)
T3-O6	1.659(1)	O9*-O6	2.734(2)	O9*-T3-O6	110.83(4)
T3-O7	1.656(1)	O9*-O7	2.771(2)	O9*-T3-O7	113.28(4)
T3-O8	1.659(1)	O9*-O8	2.849(2)	O9*-T3-O8	118.09(4)
T3-O9*	1.662(1)	O6-O7	2.628(1)	O6-T3-O7	104.90(4)
Mean	1.659(1)	O6-O8	2.641(1)	O6-T3-O8	105.48(4)
		O7-O8	2.596(1)	O7-T3-O8	103.09(4)
		Mean	2.703(1)	Mean	109.28(2)
T4-O6	1.685(1)	O10*-O6	2.781(2)	O10*-T4-O6	111.45(4)
T4-O7	1.689(1)	O10*-O7	2.776(2)	O10*-T4-O7	110.94(4)
T4-O8	1.686(1)	O10*-O8	2.856(2)	O10*-T4-O8	116.04(4)
T4-O10*	1.681(1)	O6-O7	2.671(1)	O6-T4-O7	104.70(4)
Mean	1.685(1)	O6-O8	2.683(2)	O6-T4-O8	105.48(4)
		O7-O8	2.721(1)	O7-T4-O8	107.48(4)
		Mean	2.748(1)	Mean	109.35(2)
		Lateral edges		Shared diagonal edges	
Al1-O4	1.919(1)	O4-O5	2.758(2)	O4-O10	2.440(1)
Al1-O5	1.928(1)	O4-OH1	2.756(2)	O5-O9	2.416(1)
Al1-OH1	1.921(1)	O5-OH1	2.801(2)	OH1-OH2	2.454(1)
Al1-O9	1.924(1)	O9-O10	2.800(2)	Mean	2.437(1)
Al1-O10	1.913(1)	O9-OH2	2.770(2)		
Al1-OH2	1.930(1)	O10-OH2	2.796(2)	Unshared diagonal edges	
Mean	1.923(1)	Mean	2.780(1)	OH1-O10	2.868(2)
				O4-O9	2.910(2)
				O5-OH2	2.899(2)
				Mean	2.892(1)
		Lateral edges		Unshared diagonal edges	
Al2-O4	1.914(1)	O4-O5	2.766(2)	OH1-O9	2.883(2)
Al2-O5	1.931(1)	O4-OH1	2.799(2)	O4-OH2	2.911(2)
Al2-OH1	1.931(1)	O5-OH1	2.752(2)	O5-O10	2.901(2)
Al2-O9	1.933(1)	O9-O10	2.785(2)	Mean	2.893(1)
Al2-O10	1.921(1)	O9-OH2	2.816(2)		
Al2-OH2	1.928(1)	O10-OH2	2.809(2)		
Mean	1.926(1)	Mean	2.788(1)		
		Lateral edges around vacancy			
		O4-O5	3.482(2)		
		O4-OH1	3.439(2)		
		O5-OH1	3.443(2)		
		O9-O10	3.400(2)		
		O9-OH2	3.399(2)		
		O10-OH2	3.374(2)		
		Mean	3.423(1)		
		Lateral edges		Shared diagonal edges	
Al3-OH3	1.951(1)	OH3-OH4	2.915(2)	OH3-OH6	2.717(2)
Al3-OH4	1.941(1)	OH3-OH5	2.889(2)	OH3-OH8	2.490(1)
Al3-OH5	1.945(1)	OH4-OH5	2.837(2)	OH4-OH7	2.475(1)
Al3-OH6	1.943(1)	OH6-OH7	2.889(2)	OH4-OH8	2.799(2)
Al3-OH7	1.951(1)	OH6-OH8	2.817(2)	OH5-OH6	2.542(1)
Al3-OH8	1.947(1)	OH7-OH8	2.905(2)	OH5-OH7	2.726(2)
Mean	1.946(1)	Mean	2.875(1)	Mean	2.625(1)
		Lateral edges		Shared diagonal edges	
Al4-OH3	1.950(1)	OH3-OH4	2.836(2)	OH3-OH7	2.654(1)
Al4-OH4	1.942(1)	OH3-OH5	2.914(2)	OH3-OH8	2.490(1)
Al4-OH5	1.944(1)	OH4-OH5	2.896(2)	OH4-OH6	2.780(2)
Al4-OH6	1.948(1)	OH6-OH7	2.895(2)	OH4-OH7	2.475(1)
Al4-OH7	1.946(1)	OH6-OH8	2.891(2)	OH5-OH6	2.542(1)
Al4-OH8	1.944(1)	OH7-OH8	2.810(2)	OH5-OH8	2.803(2)
Mean	1.946(1)	Mean	2.874(1)	Mean	2.624(1)
		Lateral edges		Shared diagonal edges	
Li-OH3	2.118(1)	OH3-OH4	3.200(2)	OH3-OH6	2.717(2)
Li-OH4	2.101(1)	OH3-OH5	3.142(2)	OH3-OH7	2.654(1)
Li-OH5	2.108(1)	OH4-OH5	3.220(2)	OH4-OH6	2.780(2)
Li-OH6	2.112(1)	OH6-OH7	3.163(2)	OH4-OH8	2.799(2)
Li-OH7	2.113(1)	OH6-OH8	3.249(2)	OH5-OH7	2.726(2)
Li-OH8	2.109(1)	OH7-OH8	3.242(2)	OH5-OH8	2.803(2)
Mean	2.110(1)	Mean	3.203(1)	Mean	2.747(1)

* Apical O.

1.946 Å (Table 3) for each of the two Al-rich sites. These values are compatible with the refined occupancies and are more consistent than the values of 2.125, 1.892, and 1.928 Å reported by Bailey (1975).

The mean M-O,OH bond lengths for the two octahedral sites in the 2:1 layer are 1.923 and 1.926 Å in the present study (Table 3), compared with the values of 1.932 and 1.906 Å reported by Bailey (1975). The site occupancies of both A11 and A12 are $Al_{1.0}$.

TETRAHEDRAL CATION ORDERING

The distribution of tetrahedral Al^{3+} found by Bailey (1975) suggested an asymmetric distribution of charge on the two tetrahedral sheets of the 2:1 layer (mean T-O bond lengths of 1.622 and 1.620 Å in one sheet vs. 1.652 and 1.675 Å in the other sheet). This was such a surprising but interesting result that Bailey suggested a second, more accurate, refinement was desirable for confirmation. The corresponding mean T-O bond lengths in the present study are 1.654 and 1.657 Å in the T1-T2 tetrahedral sheet vs. 1.659 and 1.685 Å in the T3-T4 tetrahedral sheet (Table 3). One tetrahedron (T4) is significantly larger than the other three. Refinement of the occupancies gave $Si_{0.49}Al_{0.51}$ for the larger T4 site relative to $Si_{0.85}Al_{0.15}$ for T1-T3.

T4 is the same site found to have the largest mean T-O bond length (1.675 Å) in the earlier study. And its position is directly tied into the ordering pattern of the interlayer cations. T4 lies directly above interlayer Li^{1+} so that it further minimizes cation-cation repulsion. T4 and Li are slightly closer together (4.349 Å), despite their larger sizes, than the pairs A13-T1 and A14-T3 (4.365 and 4.387 Å, respectively), suggesting that Li has moved slightly away from the higher-charge T2 (T2-Li = 4.375 Å) and toward T4. Other structural features consistent with an asymmetric distribution of tetrahedral Al are the greater thickness of the T3-T4 tetrahedral sheet relative to the T1-T2 sheet (2.322 Å vs. 2.251 Å, Table 4) and its closer approach to the interlayer sheet (2.680 vs. 2.755 Å).

Ideally, even smaller cation-cation repulsion should be possible with a symmetrical charge distribution of Al^{3+} in the two tetrahedral sheets within a 2:1 layer, so that an Al-rich tetrahedron could be present both below and above interlayer Li in the *Ia* structure. This does not occur in this crystal. Although the reason is not known, it should be noted that most regular interstratifications in-

TABLE 4. Summary of important structural features

	T1	T2	T3	T4
Tetrahedral compositions	$Si_{0.85}Al_{0.15}$	$Si_{0.85}Al_{0.15}$	$Si_{0.85}Al_{0.15}$	$Si_{0.49}Al_{0.51}$
Tetrahedral elongation τ (°)	111.5	111.6	114.1	112.8
Tetrahedral rotation α (°)	14.3		13.6	
Basal O corrugation Δz (Å)	0.18		0.12	

	Al1	Al2	Al3	Al4	Li
Octahedral compositions	$Al_{1.0}$	$Al_{1.0}$	$Al_{0.91}Li_{0.09}$	$Al_{0.91}Li_{0.09}$	$Li_{0.82}Al_{0.18}$
Octahedral counter-rotation (°)	7.9	7.9	3.9	3.9	0.0
Octahedral flattening ψ (°)	56.6	56.7	58.6	58.6	61.2
RMS 15 internal angles	8.7	8.8	6.4	6.6	8.2
RMS 36 external angles	5.5	5.6	4.2	4.3	5.8

Sheet thicknesses (Å)	
Tetrahedral (T1-T2)	2.251
Octahedral	2.116
Tetrahedral (T3-T4)	2.323
Tetrahedral (T3-T4) to interlayer	2.680
Interlayer	2.031
Tetrahedral (T1-T2) to interlayer	2.755
Sum	14.156

Notes: Definitions: Tetrahedral rotation angle α (°): $\alpha = \frac{1}{2}|120° - (\text{mean } O_b - O_b - O_b \text{ angle})|$. Tetrahedral elongation τ (°): $\tau = \text{mean}|O_a - T - O_b|$.

Octahedral flattening ψ (°): $\cos\psi = \dfrac{\text{octahedral sheet thickness}}{2(\text{mean M-O,OH bond lengths})}$.

Octahedral counter-rotation (°): Rotation angle of the top or bottom triangular face of an octahedron in an octahedral sheet relative to the ideal (undistorted) position. Equivalently, it is one-half of the deviation of the rotation angle between the top and bottom triangular faces relative to each other in an octahedron from 60°. Sheet thicknesses (Å): Tetrahedral: $[Z_{O_b} - \text{mean } Z_{O_aOH_n})]\cdot c \sin\beta$. Octahedral: $(\text{mean } Z_{O_aOH_n})\cdot 2\cdot c \sin\beta$. Interlayer: $(Z_M - \text{mean } Z_{OH_s})\cdot 2\cdot c \sin\beta$. Interlayer separation: $(\text{mean } Z_{OH_s} - \text{mean } Z_{O_b})\cdot c \sin\beta$. Basal O corrugation ΔZ (Å): $\Delta Z = (\max|Z_{O_b}| - \text{mean } |Z_{O_b}|) \times c \sin\beta$.

Ideal β (°): $\beta_{ideal} = 180° - \cos^{-1}\left(\dfrac{a}{3c}\right)$.

volve 2:1 layers with interlayer materials that are alternatively high-charge and low-charge, e.g., chloritic hydroxide sheets vs. smectitic hydrate sheets. Lunijianlaite is a specific example in which cookeite modules alternate regularly with pyrophyllite modules (Kong et al. 1990). Such regular alternations obviously could form more easily from precursor 2:1 layers that already have an asymmetric distribution of charge.

It cannot be stated whether or not this is an isolated example of asymmetric charge distribution. In most phyllosilicates based on 2:1 layers, the two tetrahedral sheets are required to be identical in composition and charge by the ideal symmetry. Thus, refinements based on the ideal symmetry automatically give symmetrical charge distributions. The few refinements that have been made with symmetries lower than ideal have not detected any long-range asymmetry. It is possible that (1) the high pseudosymmetry of 2:1 layers hinders detection of long range asymmetry in lower subgroup symmetry (Bailey 1975) and (2) the asymmetry may involve short-range ordering that requires detection by methods other than X-ray diffraction. One of the original reasons that refinement of the "*r*" structure of cookeite was undertaken is because the ideal polar symmetry of *Cc* allows the two tetrahedral sheets to be independent with no constraints on either tetrahedral or octahedral cation ordering.

TABLE 5. Hydrogen distances and angles

	OH-H (Å)	Tilt (°)	Angle to $+X^*$ (°)	OH-O_b† (Å)	H-O_b (Å)	OH-H-O_b (°)
H1	0.957	26.7	+58.9	—	—	—
H2	0.959	36.4	−160.5	—	—	—
H3	0.967	1.9	−94.7	2.756(O3)	1.808	165.8
H4	1.007	2.8	+103.7	2.783(O2)	1.818	159.5
H5	0.930	1.5	+41.0	2.892(O1)	1.976	168.1
H6	0.970	15.3	−120.9	2.703(O6)	1.737	174.5
H7	0.956	3.7	−63.6	2.719(O7)	1.784	165.1
H8	0.986	3.7	+74.6	2.801(O8)	1.836	165.2

* Projection of angle from $+X$ to OH-H vector (clockwise = +).
† Label of acceptor O in parentheses.

All refinements of the crystal structures of trioctahedral chlorites to date indicate disorder of the tetrahedral cations. Rule and Bailey (1987) concluded that this was the most energetically stable arrangement for the II*b* and I*b* structural types because of the relative distribution of tetrahedral and interlayer cations. In contrast, the two refinements made to date of I*a* dioctahedral chlorites have reported ordering of tetrahedral Si and Al. One is in the present study and the other in that of Aleksandrova et al. (1972), who refined the structure of donbassite, a di,dioctahedral chlorite having a distorted I*a*-2 structure, to a residual of 9.9%. Aleksandrova et al. (1972) derived the mean T-O bond lengths of 1.62 and 1.68 Å for the two tetrahedra that are independent in subgroup symmetry *C*2. The reason for this difference in ordering between type *a* and type *b* chlorites is that the "*a*" arrangement creates a close approach of a tetrahedral cation to a particular interlayer cation, whereas this is not possible in the "*b*" arrangement. The "*a*" arrangement thus allows a lower energy state to be achieved by ordering either to minimize cation-cation repulsion or to position the local source of negative charge on a tetrahedral sheet adjacent

to the local source of positive charge on the interlayer sheet.

Distortion of the structure

The "*r*" structure defined by the coordinates in Table 2 can be described by the Lister and Bailey (1967) symbols of $\bar{x}_1$-I*a*-6:$\bar{x}_2$-I*a*-6 relative to an arbitrary set of starting pseudohexagonal axes. Relative to the resultant axes, the stagger of layer 1 is $-a_2/3$ [an N layer in the terminology of Mathieson and Walker (1954)] and the staggé of layer 2 is $-a_3/3$ (an M layer). If the M layer had been taken as the first layer, the Lister and Bailey symbol would change to $\bar{x}_1$-I*a*-4:$\bar{x}_3$-I*a*-2.

To facilitate the discussion of the approximate directions of positional shift, the following noncrystallographic axes are used in this and subsequent sections: X_1, X_2, and X_3 refer to a set of three axes situated 0, 120, and 240°, respectively, counterclockwise from *a*, and *Z* is parallel to *c*. Y_1 refers to an axis situated 90° counterclockwise from X_1.

Because of the large, vacant trans octahedron in the 2:1 layer, the stagger of one tetrahedral sheet relative to the other tetrahedral sheet within the 2:1 layer is greater (0.368*a*) than ideal (0.333*a*). The sequence of displacements of the centers of six-membered rings in the structure is (1) $-0.369a$ along X_2 in the N layer, (2) an offset of $-0.335b$ along Y_3 across the interlayer, (3) a shift of $-0.368a$ along X_3 in the M layer, and (4) an offset of +0.335b along Y_2 across the next interlayer. This gives a net displacement of $-0.635a$ along X_1 and a slightly smaller β angle (96.6°) than ideal (96.93°).

The 2:1 layer is dioctahedral with the two cis octahedral sites occupied and exhibits the expected dioctahedral distortions. The vacant trans octahedral site is expanded relative to the two cis sites occupied by Al. The lateral octahedral edges are twisted, and the shared octahedral edges are shortened. The tetrahedra tilt around the vacancy causes corrugations of the basal O surface (Δz = 0.18 Å in the T1-T2 sheet and 0.12 Å in the T3-T4 sheet, Table 4) parallel to the direction of stagger within each 2:1 layer (X_2 and X_3). The angle of tetrahedral rotation α = 14.3° in the T1-T2 sheet and 13.6° in the T3-T4 sheet of the 2:1 layer. The direction of rotation moves the basal O atoms toward both the octahedral cations within the 2:1 layer and the superimposed OH groups of the interlayer sheet. An ideal tetrahedron has τ = 109.47°, which increases with elongation normal to the sheet. All tetrahedra are elongated, with T3 elongated the most (Table 4) to coordinate better with the larger, Al-rich T4 in the same sheet.

Although the interlayer hydroxide sheet is trioctahedral, it is distorted in a dioctahedral fashion because the large Li^{1+} is ordered primarily into one site. The distortion of the interlayer sheet shows the same shortening of the shared octahedral edges and twisting of lateral edges as observed in the dioctahedral sheet of the 2:1 layer, as described above. Despite the presence of the large Li^{1+} in the interlayer, the interlayer sheet is thinner (2.031 Å) than the octahedral sheet within the 2:1 layer (2.116 Å, Table 4) because of the strong attraction between the negatively charged 2:1 layers and the positively charged interlayer. As a result, the large Li octahedron is flattened (ψ = 61.2°) more than the A13 and A14 octahedra (ψ = 58.6° for each), which, in turn, are flattened more than A11 and A12 octahedra (ψ = 56.6 and 56.7°) in the 2:1 layer (Table 4). Ideal octahedra have ψ = 54.73°, which increases with flattening.

Hydrogen-bond system

The maxima of the protons on DED maps corresponded to electron values from 0.2 to 0.4, increasing in the order H5, H3, H4, H6, H8, H7, H2, to H1. The protons in this structure are all located at expected distances between 0.93 and 1.01 Å from the O atoms of their associated OH groups (Table 5). The distances from the protons of the surface OH groups to the acceptor basal O atoms are in the range 1.737–1.976 Å, forming bent hydrogen bonds with OH-H-Ob angles between 160° and 175°. These protons are tilted between 1.5° and 3.7° away from the vertical line for five of the six surface OH groups, but with a larger value, more than 15°, for H6. Joswig et al. (1980) found a tilt of 3.5° for a trioctahedral II*b*-4 chlorite studied by neutron diffraction. They also predicted the directions of proton tilt for I*a*, I*b*, II*a*, and II*b* chlorite units. In I*a* and II*a* structures, the tilting modes about interlayer cation A (which superimposes on tetrahedral cations) is different than for the two interlayer cations B [which superimpose on an inner OH group in (001) projection] to give an uneven distribution of the electrostatic field within the interlayer sheet. In the present study, cation A correlates with Li and the two B cations with Al3 and Al4. Tetrahedral cations above the interlayer superimpose on Li with an inner OH group over each of Al3 and A14. The tilting mode patterns predicted by Joswig et al. (1980) can be recognized in the cookeite "*r*" structure, but the tilted protons do not point directly toward the acceptor O atoms as predicted. This is probably due to the dioctahedral distortion of the interlayer sheet (see above), in which every large, low-charge Li^{1+} is surrounded by six smaller, high-charge Al^{3+} cations. The protons of all six independent surface OH groups coordinating the Li^{1+} are observed to tilt away from the two closest Al^{3+} neighbors towards the low-charge Li^{1+} (Fig. 1). This direction of tilt is always toward the same side of the donor OH groups as the acceptor basal O atoms, and in an ideal, undistorted structure would be at 60° from a direct line to each acceptor O. Tetrahedral rotation and octahedral counter-rotation in the interlayer shorten each O-OH hydrogen bond contact, but the O-OH pairs are affected differently because of (1) the presence of different sizes and charges of tetrahedral cations in the T3-T4 tetrahedral sheet, (2) the presence of different sizes and charges of octahedral cations in the interlayer sheet, and (3) the closer approach of the interlayer to the T3-T4 tetrahedral sheet. For example, the O-OH bond lengths for O6, O7, and O8, which form the large T4 tetrahedron

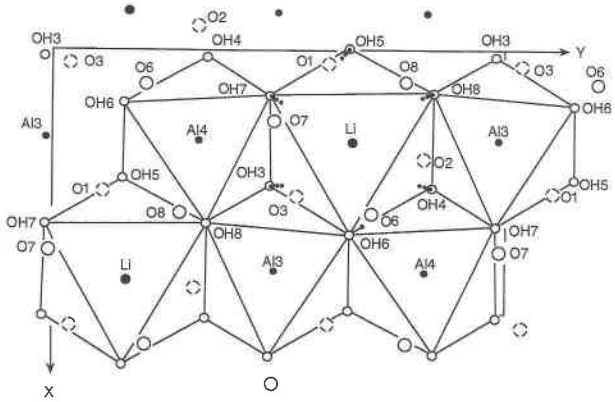

FIGURE 1. [001] projection of the interlayer sheet between an N layer (below) and an M layer (above). Solid circles = interlayer cations, large open circles = acceptor basal O atoms below (dashed) and above (full) the interlayer, small open circles = OH groups, and short dotted lines = OH-H extended vectors. H atoms are small dots inside OH circles, except for H6 whose position is between OH6 and O6.

immediately above the large interlayer Li octahedron, are smaller than those for O1, O2, and O3, which form the smaller T2 tetrahedron below Li (Table 4). X-ray diffraction is not as accurate as neutron diffraction in locating the positions of protons. But if the H sites in Table 2 are reasonable, the O6-OH6 contact is unique because it is the shortest contact (2.703 Å) and OH6-H6-O6 deviates only 5.5° from a straight line because the larger tilt (15°) of H6 toward O6. The other five contacts involve bent hydrogen bonds (Table 4) that are twisted to varying degrees toward the acceptor O atoms (Fig. 1). The bonds involving H3 and H5 are twisted considerably, whereas those involving H4, H7, and H8 are twisted very little. The longest OH-O contact distances (2.892 and 2.801 Å) involve the two basal O atoms (O1 and O8) that are buckled up or down due to tilting of the tetrahedra around the vacant octahedron in the 2:1 layer. The protons of the two inner OH groups within the 2:1 layer tilt by 27° and 36° (for H1 and H2) away from the vertical line. H1 points directly toward the vacant site, as expected, but H2 deviates from this direction by 36°.

ACKNOWLEDGMENTS

This research was sponsored in part by NSF grant EAR-8614868 and in part by grant 17966-AC2-C from the Petroleum Research Fund, administered by the American Chemical Society. We are indebted to Charles G. Stone for provision of the samples studied, to John Fournelle for the electron microprobe analysis, to the Department of Chemistry, University of Wisconsin-Madison, for use of their diffraction facilities, and to Randy Hayashi for technical assistance.

REFERENCES CITED

Aleksandrova, V.A., Drits, V.A., and Sokolova, G.V. (1972) Structural features of dioctahedral one-packet chlorite. Soviet Physics–Crystallography, 17, 456–461. (English translation by American Institute of Physics).

Bailey, S.W. (1975) Cation ordering and pseudosymmetry in layer silicates. American Mineralogist, 60, 175–187.

Bailey, S.W. and Brown, B.E. (1962) Chlorite polytypism: I. Regular and semirandom one-layer structures. American Mineralogist, 47, 819–850.

Bailey, S.W. and Lister, J.S. (1989) Structures, compositions and X-ray diffraction identification of dioctahedral chlorites. Clays and Clay Minerals, 37, 193–202.

Busing, W.R., Martin, K.O., and Levy, H.A. (1964) ORFFE, a Fortran crystallographic function and error program. Oak Ridge National Laboratory Technical Manual, 306, 83 p.

Černý, P. (1970) Compositional variations in cookeite. Canadian Mineralogist, 10, 636–647.

Joswig, W., Fuess, H., and Rothbauer, R. (1980) A neutron diffraction study of a one-layer triclinic chlorite (penninite). American Mineralogist, 65, 349–352.

Kong, Y., Peng, X., and Tian, D. (1990) Lunijianlaite—a new regular interstratified mineral: Acta Mineralogica Sinica, 10, 289–298 (in Chinese).

Lister, J. and Bailey, S.W. (1967) Chlorite polytypism: IV. Regular two-layer structures. American Mineralogist, 52, 1614–1631.

Mathieson, A.M. and Walker, G.F. (1954) Crystal structure of magnesium-vermiculite. American Mineralogist, 39, 231–255.

Peacor, D.R., Rouse, R.C., and Bailey, S.W. (1988) The crystal structure of franklinfurnaceite: A tri–dioctahedral zinc silicate intermediate between chlorite and mica. American Mineralogist, 73, 876–889.

Rule, A.C. and Bailey, S.W. (1987) Refinement of the crystal structure of a monoclinic ferroan clinochlore. Clays and Clay Minerals, 35, 129–138.

Stone, C.G. and Milton, C. (1976) Lithium mineralization in Arkansas. United States Geological Survey Professional Paper, 1005, 137–142.

MANUSCRIPT RECEIVED MAY 2, 1996
MANUSCRIPT ACCEPTED APRIL 23, 1997